Journal of Magnetic Resonance Open 8–9 (2021) 100017

Contents lists available at ScienceDirect

Journal of Magnetic Resonance Open

journal homepage: www.sciencedirect.com/journal/journal-of-magnetic-resonance-open

An automated system for fast transfer and injection of hyperpolarized solutions

Morgan Ceillier [a,*], Olivier Cala [a], Théo El Daraï [a], Samuel F. Cousin [a], Quentin Stern [a], Sylvie Guibert [a], Stuart J. Elliott [a,b], Aurélien Bornet [c], Basile Vuichoud [a], Jonas Milani [c], Christophe Pages [d], Dmitry Eshchenko [e], James G. Kempf [f], Catherine Jose [d], Simon A. Lambert [g], Sami Jannin [a]

[a] *Center de Résonance Magnétique Nucléaire à Très Hauts Champs, UMR 5082, Université Claude Bernard Lyon 1 / CNRS / ENS de Lyon, 5 Rue de la Doua, Villeurbanne 69100, France*
[b] *Department of Chemistry, University of Liverpool, Liverpool L69 7ZD, United Kingdom*
[c] *Ecole Polytechnique Fédérale de Lausanne, Institut des Sciences et Ingénierie Chimiques, Lausanne 1015, Switzerland*
[d] *Institut des Sciences Analytiques, UMR 5280, Université de Lyon / CNRS / Université Claude Bernard Lyon 1 / ENS de Lyon, 5 rue de la Doua, Villeurbanne 69100, France*
[e] *Bruker Biospin, Fallanden 8117, Switzerland*
[f] *Bruker Biospin Corp., Billerica, MA 01821, United States*
[g] *Laboratoire Ampère, UMR 5005, USC 1407, Ecole Centrale de Lyon / INSA de Lyon / Université Claude Bernard Lyon 1 / CNRS, 36 Avenue Guy de Collongue, Ecully 69134 Cedex, France*

ARTICLE INFO

Keywords:
NMR
Hyperpolarization
dDNP
Dissolution
Instrumentation
Transfer

ABSTRACT

Dissolution dynamic nuclear polarization (*d*DNP) has become a hyperpolarization method of choice for enhancing nuclear magnetic resonance (NMR) signals. Nuclear spins are polarized in solid frozen samples (in a so-called polarizer) that are subsequently dissolved and transferred to an NMR spectrometer for high sensitivity detection. One of the critical challenges of *d*DNP is that it requires both a fast transfer to limit nuclear spin relaxation losses as well as stability to guarantee high resolution (no bubbles nor turbulences). Here we describe the design, construction and performances of such a transfer and injection system, that features a 5 m/s speed and sub-Hz spectral resolution upon arrival at the detection spot. We demonstrate the use of such a system for inter-magnet distances of up to 10 m.

Introduction

Nuclear magnetic resonance (NMR) in the liquid-state proves to be one of the most powerful tool for analytical chemistry, metabolomics, drug discovery, and many other fields of research [1–5]. However, its inherent lack of sensitivity can sometimes be a severe drawback, such as for studying low concentrated molecules with naturally abundant ^{13}C [6]. To address this issue, several hyperpolarization methods have been developed [7], among which is dissolution dynamic nuclear polarization (*d*DNP) [8,46]. In a standard *d*DNP experiment, samples made of solutions of molecules mixed together with polarizing agents (PAs) are loaded in the liquid helium bath of a *d*DNP polarizer providing a moderate magnetic field and low temperature environment (typically 3.35-7 T and 1-4.2 K). The sample is then irradiated with microwaves near the electron spin resonance (ESR) frequency of the PAs as a means of transferring the high electron spin polarization to the surrounding nuclear spins. Polarization values typically close to 90% can be attained for ^{1}H spins [9–11] while polarization values typically larger than 50% can be achieved on low-gamma nuclear spins using direct [12,13] or cross-polarization [9,14] assisted DNP. The frozen sample is then generally dissolved using a hot pressurized solvent and transferred through a capillary with pressurized gas into a nearby NMR or magnetic resonance imaging (MRI) machine for acquisition in typically ~10 s, resulting in enhancements of 4 to 5 orders of magnitude with respect to thermal equilibrium signals. However, this method has several limitations that hamper its routine use in several applications. First, transfer times can lead to substantial polarization losses for fast relaxing nuclear spins. Second, passage through low-field regions can accelerate this loss

* Corresponding author.
E-mail address: morgan.ceillier@univ-lyon1.fr (M. Ceillier).

https://doi.org/10.1016/j.jmro.2021.100017
Received 6 May 2021; Received in revised form 16 July 2021; Accepted 23 July 2021
Available online 1 August 2021

of polarization through enhanced relaxation [15] or even through level anti-crossing or coherent effects [16–18]. Third, substantial variations in NMR signal intensities can arise from one dissolution to the other if sample transfer and injection is not sufficiently repeatable. Last, significant line broadening can arise if the injection is turbulent or if gas bubbles remain present in the NMR tube after injection.

Several groups have contributed to improving dissolution, transfer and injection. By adjusting gas pressure and transfer capillary diameters, Granwehr et al. [19] reported transfer times of ~2.5 s over 5.6 m, and the group of Frydman [20] reported transfer times of 1.2 s resulting in ^{1}H enhancements of ≈ 500 on a 500 MHz NMR spectrometer. A significant advance was brought by the group of C. Hilty who proposed a design where the dissolved sample was first loaded in a dedicated transfer setup based on an HPLC valve, and then transferred at high speed using nitrogen gas. [21] This fast transfer system was already adapted in other laboratories [22,23] and was further modified to integrate a liquid pump for liquid-driven transfer. [24,25] Such sophisticated systems reached transfer times of 700 ms, which turned out to be a game changer for hyperpolarized ^{1}H detection. [26,27] However, in all of these studies, the polarizer and the NMR spectrometer were placed very close to one another, with typically less than three meters of total capillary lengths.

In most laboratory configurations, several NMR spectrometers could benefit from hyperpolarization from the same *d*DNP polarizer, but all cannot be placed at minimal distance from it, particularly if some of the magnets are not ultra-shielded. In our laboratory, distances between our polarizer and the liquid-state NMR spectrometers around (ranging from 80 MHz to 1 GHz) are typically between 2 and 20 m. Transferring hyperpolarized samples over such long distances not only results in longer transfer times, but also in different fluidic dynamics with substantial pressure drops and increased turbulences. This causes several issues such as the increased presence of bubbles, decreased repeatability in the injected volume, etc. In the case of gas-driven transfers, during the transfer of the liquid plug of hyperpolarized sample, the plug of dissolved sample rapidly breaks and takes the form of a thin layer on the wall of the transfer tube, which ends up in an inefficient and unrepeatable transfer and injection volume and timing. The film thickness depends on the speed and length of the transfer, implying that for faster transfer over a longer distance, the liquid plug loses most of its speed and final volume along the way [28–31]. Furthermore, turbulences induce a mixing between gas and liquid, forming bubbles in the plug. Such heterogeneous plugs lead to poor injection repeatability, sometimes with bubbles in the detection area of the NMR coil [19,22,23] affecting the resolution of the acquired NMR spectra. For liquid-driven transfer [24], high turbulences due to high speed and long distance induce a mixing between the pushing liquid and the dissolved sample [32]. Under certain speed and turbulence conditions, the driving liquid may even contaminate the whole liquid plug and thus the final injected sample. However, such liquid-driven transfer has the potential to improve the injection performances if compared to gas-driven transfer (faster, better repeatability, etc.) because it prevents the problem of air bubbles and offers perspectives of higher speed transfers and better controlled stabilization.

Here, we propose and describe in detail the design of a rapid transfer and injection system that can be adapted to any *d*DNP polarizer coupled to NMR spectrometers located at short to long distances (at least up to 10 m). We describe critical inherent fluid mechanics issues of such fast transfers over long distances and present a detailed optimization of the whole setup. Finally, we present the associated performances, with transfer speeds of typically 5 m.s^{-1}, and sub-Hz linewidths after injection.

Methods

The liquid-driven home-built dissolution and transfer system (see Fig. 1(a)) is coupled with a Bruker Biospin Prototype *d*DNP polarizer

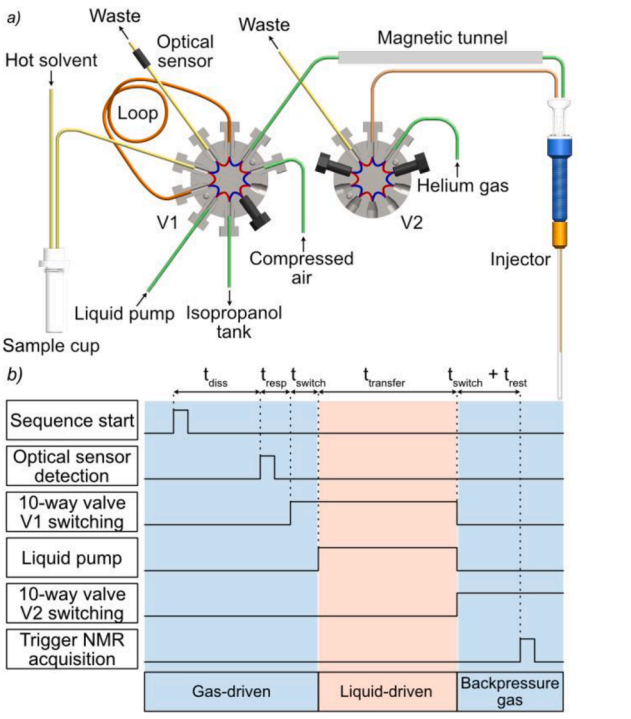

Fig. 1.. (a) general setup of the dissolution and transfer system. Note that the black screws on the 10-way valves are plugs – (b) sequence timing of the dissolution and transfer process, with t_{diss} = 1351 ms, t_{resp} = 8.4 ms, t_{switch} = 50 ms, $t_{transfer}$ = 2100 ms and t_{rest} = 0 ms in our case (For interpretation of the references to color in this figure, the reader is referred to the web version of this article.).

(AlphaPolarizer) that we equipped with a home-built sample cup and holder as well as a coupling stick for dissolution. The transfer system comprises two 10-way fast switching valves (V1 and V2), an optical sensor, a high-pressure high-flow liquid pump, and a home-built magnetic tunnel. The design resembles the one described by Hilty's group, [24] with a number of differences detailed in the hardware section, The injection system is composed of a home-built 3D-printed NMR tube holder. The different parts are linked together using capillaries made of either PTFE or PEEK tubing with 1/8" outer diameter (o.d.) and 1/16" inner diameter (i.d.).

Control system

The dissolution and transfer systems are controlled by a home-built electronic system based on a CompactRIO card (cRIO-9068, National Instruments, Austin, TX), and a LabVIEW interface (available upon request). At first, 7 mL of solvent, usually D_2O, is inserted in the dissolution box (see Section "Dissolution box"), pre-pressurized at 6 bar with helium gas and warmed up until the internal pressure reaches 9 bar (≈ 175 °C). Once the dissolution stick is manually coupled to the sample cup, the dissolution is triggered by pressing a button integrated in the handle of the dissolution stick. The dissolution box lower pneumatic valve is opened to release the hot pressurized solvent onto the frozen sample, and the upper valve is opened (typically after 700 ms) to push the dissolved sample through the output capillary of the dissolution stick with 6 bar of helium gas. The dissolved sample enters the first 10-way valve V1 (AL10UW, VICI AG International, Schenkon, Switzerland) (see Fig. 1(a) and fills a 1.5 m long PTFE capillary (1/8" o.d., 1/16" i.d., 189503, Interchim, Montluçon, France) used to select a plug of hyperpolarized liquid with a predefined volume of 3 mL. An optical sensor (OCB350L125Z, TT Electronics/OPTEK Technology, Woking, United Kingdom), placed 41 cm after V1, detects the presence of liquid, which indicates that the loop is filled. The time t_{diss} necessary for the hot

solvent to melt the sample and be detected by the sensor (see Fig. 1(a) and (b)) is typically less than 1.5 s. Upon sensor detection, V1 is switched, connecting the loop both to a liquid pump and to the capillary going through a magnetic tunnel [33], and the liquid pump (mzr-11508 × 1 S, HNP Mikrosysteme GmbH, Schwerin, Germany) is triggered. Considering the system response time $t_{resp.}$ that includes the optical sensor response time (3 ms) and the software reaction time (5.4 ms), the time taken for the valve to switch including the electro-distributor (t_{switch} = 50 ms), and the pump response time (15 ms), one can make the approximation that the transfer starts roughly 75 ms after the liquid arrival at the optical sensor.

The pump delivers a chosen volume of isopropanol at a chosen flow rate, which provides a way of transferring and injecting 540 μL of hyperpolarized sample in the NMR tube in a reproducible way, in a time $t_{transfer}$. At this point, an exhaust tubing plugged onto the 3D-printed NMR tube holder (drawings available upon request) is connected to a waste container through the second 10-way valve V2. Just after the liquid pump finishes transferring the dissolved sample, V2 is switched, connecting the exhaust capillary of the NMR tube holder to a line of helium gas with 6 bars of pressure. This backpressure prevents degassing to happen in the injected sample, which can be very detrimental to the NMR resolution, with substantial inhomogeneous line broadening. The backpressure of 6 bars was chosen for simplicity since it was readily available in our laboratory, and gave satisfactory results. Further optimization might lead to faster stabilization and improved linewidths after injection (see Results section). V1 is also switched back into its original position to prevent any backflow through the magnetic tunnel. Finally, after an additional time t_{rest} to allow the injected liquid to stabilize, the NMR spectrometer receives a trigger from the dissolution control system for signal acquisition. Fig. 1(b) shows the sequence timing.

Polarizer and NMR spectrometer

The Bruker Biospin *d*DNP prototype polarizer AlphaPolarizer is operating at a field of 7.05 T (corresponding to a ^{1}H Larmor frequency of 300 MHz) and temperatures down to 1.2 K. A microwave source (Virginia Diodes Inc., Charlottesville, VA) is used, operating in the range 196.8–198.8 GHz with a power of ca. 125 mW at the output of the amplifier module, and ca. 30 mW reaching the sample. The hyperpolarized liquid-state NMR experiments are conducted on a Bruker Biospin Fourier 80 benchtop magnet operating at 1.88 T (corresponding to a ^{1}H Larmor frequency of 80 MHz). The benchtop magnet was customized by Bruker Biospin to compensate for excessive drop of stray field (see more details in Fig. 3) which would lead to polarization losses during transfer.

Dissolution box

The dissolution box provides hot pressurized solvent needed for the dissolution of the sample and from a functional point of view is similar to reference [8]. It consists of Swagelok components, including 10 mL 316 stainless-steel sample cylinder, digital pressure transducer, two automated diaphragm-sealed 316 stainless-steel valves (one, connected to the top of the cylinder, for pressurization with helium gas, one for releasing the warm solution towards the sample cup) and a manual 316 stainless-steel valve for refilling the cylinder with the solvent (e.g. D_2O). Solvent is inserted in the cylinder through the manual valve using a syringe extended by a 1/16'' i.d. and 1/8'' o.d. PEEK capillary. The cylinder is wrapped with a 20 Ω heater connected via computer-controlled solid-state relay to a powerful 24 V supply. The temperature of the cylinder is monitored by a standard PT1000 sensor. The pressure of the solvent is controlled via simple heater on/off algorithm.

Sample cup and dissolution stick

The sample cup (see Fig. 2(a) and (b)) is machined in PEEK, and has an i.d. of 6.3 mm. It is made to center up to 200 μL of sample in the sweet spot of the polarizer. The lower longer part has an o.d. of 8.3 mm and has a M10*1mm thread over 2 mm. A 16 mm o.d. stainless steel tube with 0.3 mm wall thickness (2250300312, Harry Rieck GmbH, Hilden, Germany) with a 3.5 mm thick washer soldered at the bottom and its internal M10*1 mm thread are used to place the sample cup in the liquid helium bath of the polarizer. Correct positioning and alignment of the sample cup are guaranteed by screwing it to the washer manually. A DN16 ISO-KF half nipple is soldered at the top of the sample tube and an o-ring and blank flange (Pfeiffer Vacuum, Annecy, France) are used to make the polarizer leak tight during the DNP process. Before dissolution, the o-ring and blank flange are removed and the coupling stick is inserted in the sample tube. The coupling stick, also called the dissolution stick, contains a stainless-steel tube (13.37 mm o.d., 12.37 mm i.d., 304L, Inoxtube, Coulommiers, France) in which two PEEK capillaries (1/8" o.d., 1/16" i.d., 803776, Interchim, Montluçon, France) are inserted. Those capillaries are connected at the bottom of the dissolution stick to a PEEK part, dubbed here the dissolution interface. The dissolution interface, inserted in the 13.37 mm o.d. tube, is the part that couples to the sample cup, allowing the hot solvent to come in through one of the capillaries, dissolve the sample, and then be pushed away through the other capillary. Two 1.6 mm holes link the capillaries to the sample cup. The input capillary is glued (Super Glue-3, Loctite, Henkel, Düsseldorf, Germany) around a smaller stainless-steel capillary (1/16" o.d., 1.17 mm i.d., 572170, Interchim) that goes through the dissolution interface, decreasing the inner diameter of the fluid path on the way in. The output and input capillaries are both glued to the dissolution interface, also using Super Glue-3. The coupling is made leak tight simply by machining the same diameter on both on the outer upper part

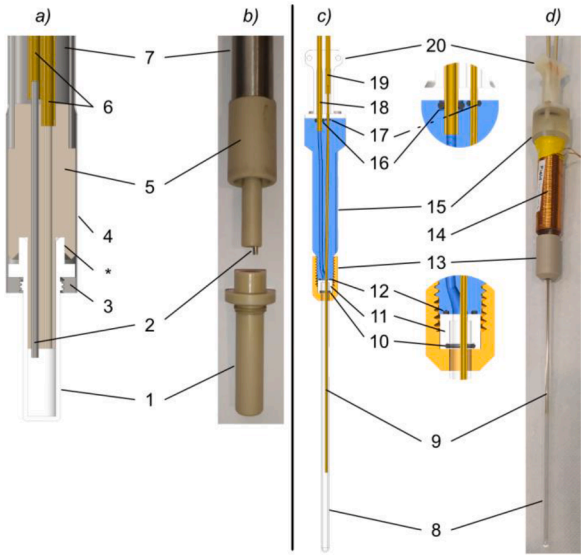

Fig. 2.. (a) 3D model and (b) photo of the dissolution stick and sample cup, comprising a PEEK sample cup (1), a 1/16'' o.d. stainless steel tube (2), a washer with screwing hole (3), a 16 mm o.d. stainless steel tube (4), a PEEK dissolution interface (5), two 1/8'' o.d. and 1/16'' i.d. PEEK tubes (6) and a 13.37 mm o.d. stainless steel tube (7). (*) shows the area made leak tight by the coupling. (c) 3D model and (d) photo of the injector, comprising a 5 mm NMR tube with 3.4 mm i.d. (8), a tube head in PEEK (11), a 1/16'' o.d. and 1 mm i.d. PEEK tube (9), three o rings with 1 mm cross section and 5 mm i.d. (10) – 5.5 mm i.d. (12) – 1/16'' i.d. (17), a custom PEEK nut (13), a solenoid (14) wired on a 3D-printed custom spinner (15), an o ring with 1/16'' cross section and 1/8'' i.d. (16), two 1/8'' o.d. PEEK tubes with 2.2 mm i.d. (18) and 1/16'' i.d. (19), and a 3D-printed plug (20) (For interpretation of the references to color in this figure, the reader is referred to the web version of this article.).

of the sample cup and the inner part of the dissolution interface, as shown in Fig. 2 (a). The thermal shrinkage of the low temperature sample cup makes the coupling possible. On top of the dissolution stick is a 3D-printed custom handle (SLS, Nylon PA-12, Sculpteo, Villejuif, France), glued to the 13.37 mm o.d. tube using an epoxy glue (Armstrong A-12, Henkel, Düsseldorf, Germany). Beside its obvious function of holding the dissolution stick during the coupling step, the handle also includes a button (AV51222000074BK, APEM, Caussade, France) used to manually trigger the dissolution and transfer sequence. It also has a hole, allowing both capillaries to come out of the dissolution stick and be connected to the dissolution box for the input capillary and to the 10-way valve V1 for the output capillary. A home-built solenoid, detailed in Section "Solenoids", is also added around the output capillary to prevent the hyperpolarized dissolved sample traveling through low field regions. Both the solenoid and the button are soldered inside the handle to a connector (T3507000, Amphenol, Wallingford, CT). A cable connected to the acquisition card is then plugged to this connector to power the solenoid and the button. It should be noted that the system has been working for two years with several hundreds of experiments performed without a single leakage or breakage of the sample cup in the polarizer.

10-way valves

The 10-way valves (AL10UW, VICI AG International, Schenkon, Switzerland) used here are air-actuated valves that can switch between two positions, as indicated by the blue and red lines of Fig. 1 (a). They can in principle operate at pressures up to 345 bar. A high-speed switch accessory (HSSA, VICI AG International, Schenkon, Switzerland) is added on each valve, to decrease the switching time down to 8 ms (measured to be 6.6 ms in practice), using helium gas as the gas actuator.

Optical sensor

An optical sensor is used to detect liquid (OCB350L125Z, TT Electronics/OPTEK Technology, Woking, United Kingdom). Using an LED and a phototransistor, it detects the presence of air or liquid in clear tubing only (1/8" o.d.) with a typical detection time of 3 ms. Therefore, PEEK tubing cannot be used here as those are opaque, and a PTFE tubing is preferred.

Liquid pump

The pump used to push the dissolved sample to the NMR spectrometer is a micro-annular gear pump (mzr-11508 × 1 S, HNP Mikrosysteme GmbH, Schwerin, Germany). It is a programmable pump that can produce a relatively high flow, up to 1152 mL.min^{-1}, that is well suited for long distance transfer. It can withstand output pressures up to 40 bar, and the speed of the pump (max. 6000 rpm) as well as the number of turns can be set for the pump to deliver a target volume upon triggering. The liquid chosen for pushing the dissolved sample is isopropanol (10674732, Fisher Scientific SAS, Illkirch, France) as it prevents the development of microorganisms in the pump, but water could equally be used together with a regular cleaning procedure.

Magnetic tunnel

To help maintain hyperpolarization in the liquid state during the transfer, a magnetic tunnel has been installed between the polarizer and the NMR spectrometer. Its design is similar to a previous study [33] but has been made compatible with 3D-printing technology. The four rows of permanent magnets (5*5*100 mm, neodymium, N52, nickel-plated, Supermagnete, Gottmadingen, Germany) composing the Halbach configuration produce a transverse magnetic field of 0.75 T, with drops to 0.5 T at the angles of the tunnel. The total length of the tunnel is 6.98 m. The capillary that goes through the tunnel is a 9.44 m long PEEK tube with 1/8'' o.d. and 1.16'' i.d.

Solenoids

Low magnetic fields can lead to exacerbated polarization losses and should be avoided. For example, with our customized Bruker Biospin Fourier 80 benchtop magnet, the stray field is smaller than 1 mT at the bore entrance, see Fig. 3(a). Therefore, solenoids have been added at strategic places along the fluid path. The solenoids were added at (i) the output capillary of the dissolution stick going to the 10-way valve V1, (ii) the beginning of the tunnel capillary from the 10-way valve V1 to the start of the magnetic tunnel, (iii) the end of the tunnel capillary from the end of the magnetic tunnel to the injector, and (iv) the injector main body part. Also, larger diameter solenoids have been placed (v) at the

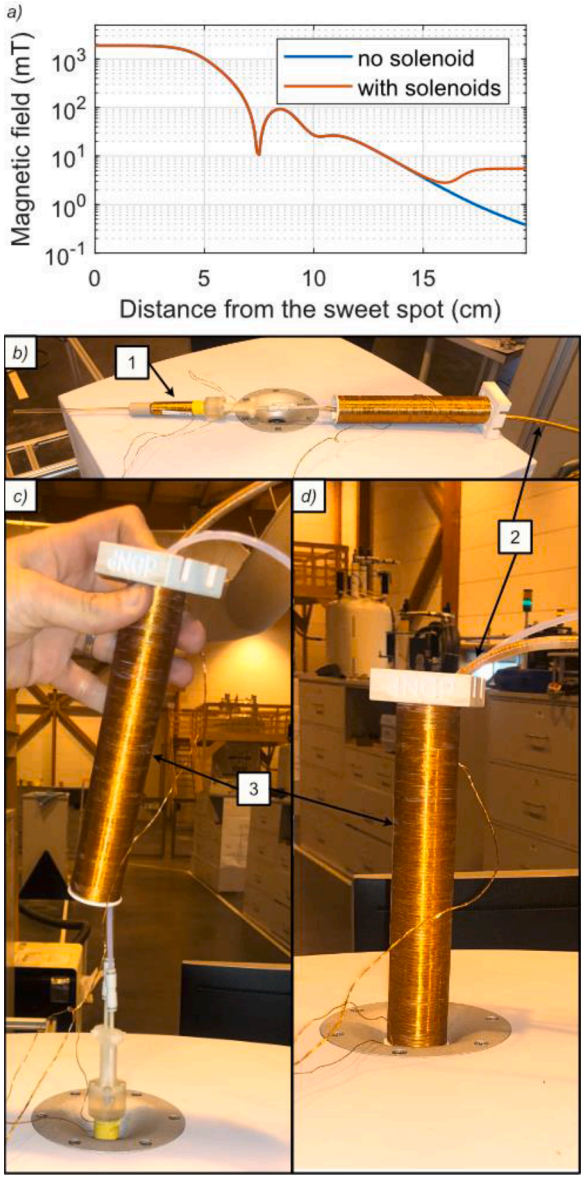

Fig. 3.. (a) Stray field of the customized Bruker Biospin Fourier 80 benchtop magnet from the sweet spot along the *z* axis, with and without the solenoids (1) and (3). The blue curve is based on Bruker Biospin data, and the added solenoid fields are based on infinite solenoids theory. Pictures of the three solenoids used at the injector side to avoid low field regions during the transfer: (1) on the injector, (2) at the end of the tunnel capillary and (3) around the junction of the other two. (b) is a disassembled view, (c) shows the injector inserted in the benchtop and (d) shows the assembled setup (For interpretation of the references to color in this figure legend, the reader is referred to the web version of this article.).

interface of the solenoids and the permanent magnets at the beginning and the end of the magnetic tunnel, and (vi) at the interface of the injector and the end of the tunnel capillary. All the solenoids are wired using 0.5 mm diameter copper wire (357-744, RS PRO, Beauvais, France). With a current of 2.5 A applied, it ensures a sustained magnetic field of approximately 5 mT. Fig. 3(b) to (d) shows the solenoids used on the injector side.

Injector

The NMR tube holder, in which the hyperpolarized solution is injected for acquisition, is presented Fig. 2 (c) and (d), and is called here the injector. A medium-wall NMR tube (5 mm o.d., 3.4 mm i.d., 524-PP-7, Wildmad-LabGlass, Vineland, NJ) that can withstand 10 bars of pressure is cut to a total length of 165.5 mm. To ease the injection and prevent the formation of gas bubbles, the NMR tube is treated with Hellmanex^{TM} III (Hellma GmbH & Co. KG, Müllheim, Germany) by filling it with a solution of Hellmanex^{TM} III/demineralized water (1:49, *v/v*) at 40 °C for 40 min. The 1/8" o.d. PEEK capillary through which the solution is injected is glued with Super Glue-3 onto a 1/16" o.d. PEEK capillary (1 mm i.d.) above the injector. This reduction in diameter is done to prevent the 1/8" o.d. PEEK capillary from occupying most of the section of the 3.4 mm i.d. NMR tube, which would almost block the exhaust of the injection. This 1/16" capillary ends 7 cm above the bottom of the NMR tube, which was found to be optimal for water-based solution injection. The NMR tube is glued using Armstrong A-12 epoxy glue to a PEEK cylindrical part, shown in white in the Fig. 2 (c), here called the tube head. The tube head is held in position by compressing it to the custom spinner, represented in blue, using a custom nut of M12*1.75 mm (shown in gold colour) machined in PEEK. The custom spinner is 3D-printed (STL files available upon request) using a Form 3 and a clear resin V4 (Formlabs Inc., Somerville, MA) with a resolution of 25 μm. This spinner dimensions are specific for the Bruker Biospin Fourier 80 benchtop magnet but could easily be adapted for any spectrometer. It contains a curved hole of 1.8 mm i.d. for the 1/16" capillary to go through, and a 2.2 mm i.d. curved hole for the exhaust. A 2.2 mm i.d. PEEK capillary (1/8" o.d.) is inserted at the top of the spinner to take in the exhaust. The whole injector is made leak tight by compressing o-rings at several locations: a 1/16" i.d. and 1 mm cross-section (CS) is used at the top of the spinner around the 1/16" o.d. capillary, a 1/8" i.d. (1/16" CS) is placed around the 1/8" exhaust capillary, a 5.5 mm i.d. (1 mm CS) is put between the tube head and the spinner, and a 5 mm i.d. (1 mm CS) is used between the tube head and the NMR tube. All o-rings are squeezed with a 30 % compression ratio, and are made of nitrile (Polymax Ltd, Bordon, United Kingdom). A 3D-printed plug (PLA, 1.75 mm, Raise3D N2, Irvine, CA), presented in white in Fig. 2(c), is screwed onto the custom spinner to prevent the two upper o-rings from going out of their grooves. This part also tightens the input and output 1/8" capillaries using M3 nylon screws to prevent them from popping out of the injector when the backpressure is applied. Finally, considering the low stray field of the Bruker Biospin Fourier 80 benchtop magnet, a solenoid is wired around the 3D-printed spinner, as shown in Fig. 2(d), to produce a 5 mT magnetic field during injection.

Sample preparation and freezing process

The sample used for *d*DNP experiments is a mixture of H_2O:D_2O: glycerol-d_8 (1:4:5 *v/v/v*) doped with 25 mM of TEMPOL radicals. The following ^{13}C-labeled molecules are added to the mixture: 1-^{13}C-acetate (100 mM), ^{13}C-formate (100 mM), ^{13}C-urea (100 mM) and 1-^{13}C-alanine (100 mM). After sonicating the resulting solution, 100 μL was inserted in the sample cup, and the latter was shortly centrifuged to ensure that the whole sample was positioned at the bottom of the sample cup. Finally, the sample was flash-frozen directly in the liquid helium bath of the polarizer. It should be noted that the sample cup is manually immersed in liquid helium in roughly three seconds, which could in principle be compatible with the use of UV generated radicals or frozen beads.

DNP experiments

DNP was performed by shining frequency modulated microwave irradiation at 197.648 GHz ± 144 MHz, with a frequency modulation of 500 Hz, onto the sample. Cross polarization (CP) was used to transfer hyperpolarization from ^{1}H to ^{13}C nuclei using a protocol detailed elsewhere [14,34]. Eight 6.5 ms CP contacts were performed with a 5 min interval to allow enough time for the protons to repolarize between CP contacts.

Cleaning protocol

Before each dissolution experiment, all tubing are cleaned with four cycles of flushing with 5 mL of H_20 followed by 30 s of compressed air drying. A final cycle of flushing with 5 mL of H_2O followed by 2 min of compressed air drying is done. This procedure proved to remove all traces of isopropanol and sample from one dissolution to another over the 9.41 m long transfer length. The sample cup and NMR tube are cleaned by filling/emptying with H2O three to five times and finally drying with compressed air.

Results

Fluidic dynamics

Liquid-driven transfer was preferred over gas-driven transfer over the 9.5 m long capillary because it is otherwise impossible to provide consistently clear sample plugs without the presence of gas bubbles to the injector. This is a strong requirement for high resolution NMR and good repeatability. If gas bubbles are mixed with the dissolved sample plug, it becomes impossible to inject a precise volume. When pushing with gas, (i) bubbles will mix with the sample plug, and (ii) the plug volume will decrease by leaving a trail on the capillary wall. Furthermore, gas is highly compressible and one can make the approximation that liquid is not. Therefore, when the injection stops, the plug might still be pushed by the decompressing gas, which is not observed with liquid. In order for the transfer and injection to be truly repeatable, it primarily requires the loop to be filled as a single solution plug without bubbles before the pump is triggered.

Proper filling of the loop

Gas bubbles can mix with the sample liquid plug, in particular at places where the flow is very turbulent. The sample cup can be a spot of strong mixing, especially on designs with large dead volumes (typ. up to ~2 mL) filled with helium gas before dissolution. Indeed, the dissolution process is very turbulent with hot dissolution liquids entering at high speed, and gas bubbles can mix during this process. To prevent this phenomenon, we propose a design where the dead volume in the sample cup is decreased to its minimum (see Fig. 2 a). A volume of only 275 μL remains above the 200 μL of sample for the dissolution to take place. This volume could be further optimized, however the current design provided satisfactory results.

During the dissolution process, the hyperpolarized liquid plug is pushed toward the loop. The proper filling of the loop, without the presence of gas bubbles, can be checked with the optical sensors presented in Section "Optical sensor". Their output voltage depends on the amount of light received by the phototransistor. Once calibrated, the presence of liquid leads to an output of roughly 5 V as our solvent refractive index is close to the one of the PTFE tubing used. The presence of air or helium gas will lead to a lower voltage of around 2.6 V. Fig. 4 shows a typical output data set from an optical sensor when a 7 mL volume of water is pushed through it with 6 bar of helium gas. The data were recorded with an oscilloscope (DSOX1204A, 70 MHz, Keysight

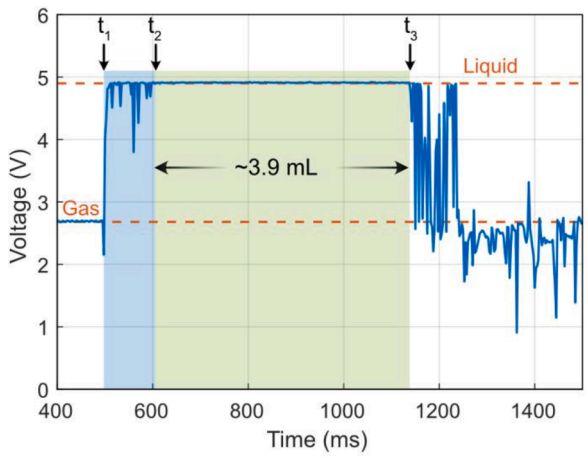

Fig. 4.. Classical data set of a OCB350L125Z optical sensor when a 7 mL volume of water is pushed through it with 6 bar of helium gas. The 5 V state indicates the presence of pure liquid, and the 2.6 V state indicates the presence of pure gas. A mix of gas and liquid leads to additional fluctuations in the measured voltage (For interpretation of the references to color in this figure, the reader is referred to the web version of this article.).

Technologies, Les Ulis, France). At t_1, the front of the liquid plug is detected at the optical sensor position. One can see that the first part of the plug, from t_1 to t_2 (indicated in blue in Fig. 4), contains a mix of gas and liquid because the voltage is observed to fluctuate. However, as shown in green in Fig. 4, starting at t_2 up to t_3, the voltage is constant, indicating a clean sample plug of liquid of roughly 3.9 mL that can therefore be properly selected for further transfer to the NMR spectrometer. The last part of the sample is a long succession of small droplets coming from the trail of liquid left on the capillary walls and pushed by the helium gas.

It becomes possible with such data sets to carefully adjust the optical sensor position so that it detects liquid when the loop is bubble-free. In our system, with the solvent being pre-pressurized with 6 bars in the dissolution box, warmed up to 9 bars and pushed with 6 bars, we found that 7 mL of solvent and the optical sensor being placed 41 cm after the loop give a gas bubble-free loop in a robust and repeatable manner.

Contamination-free transfer

The pump speed must be carefully optimized for two reasons. First, the pressure increases with faster transfer and may reach the maximum pressure accepted by the pump. Second, a mix may occur between the driving and driven liquids. This problem can be very detrimental to such extent that with long capillaries and under certain turbulence conditions, the driving liquid can even contaminate/dilute the whole hyperpolarized sample plug and be detected in the NMR spectrometer. This contamination can be a major drawback for many applications, such as metabolomics or drug screening. Key parameters for such issue are (i) the i.d. of the capillary going through the magnetic tunnel, (ii) the flow rate of transfer, (iii) the total time of transfer, and iv) the length of the sample plug that needs to be preserved from contamination. For a given capillary length, the pump will have to provide less volume of driving liquid with smaller i.d., which will enable faster transfer with reduced turbulences. However, using smaller i.d. also results in dramatically increasing the pressure, which calls for limiting the speed of the pump and therefore increasing the transfer time. Therefore, a compromise between all the counteracting parameters has to be found in order to transfer at maximum speed while ensuring zero-contamination in the NMR tube. It is worth mentioning here that the inner diameter of the 10-way valve is 1 mm, and the i.d. of the loop and of most capillaries used is 1/16''. This change of diameter may induce turbulences and mixing, but the i.d. of the 10-way valve can only be kept fixed here.

Five different transfer tube i.d. were tested: 1/16" (≈ 1.6 mm), 1.4 mm, 1.2 mm, 1 mm and 0.75 mm. The 1/16'' i.d. has a 1/8" o.d., the 1.2 mm i.d. has a 1.8 mm o.d., and the other three have a 1/16'' o.d. The five tubes had a 9.41 m length. For each tube, the following experiment was conducted: the tube was first connected directly on the 10-way valve to replace the capillary going through the magnetic tunnel. The injector described previously was connected at the other end of the tube. The loop was then filled manually with H_2O. The pump was triggered to inject 540 μL into the NMR tube. Next, a ^1H spectrum was acquired on a Bruker Fourier 80 benchtop spectrometer to quantify the amount of contaminating isopropanol. Finally, all tubing were cleaned thoroughly with H_2O and dried with compressed air. The experiment was then repeated with an increased speed of the pump, until the maximum pressure accepted by the pump was reached (limited here to 37.5 bar). The results are presented in Fig. 5. Fig. 5 (a) shows the transfer time depending on the speed of the pump, for each i.d. Note that the curves are only a guidance for the eye. The volume that the pump needs to displace in order to transfer the liquid is reduced for smaller i.d. since the internal volume of the tube is smaller. Therefore, for a given pumping speed, the transfer is faster for small i.d. The smaller graph of Fig. 5 (a) is a zoom in the region of the faster transfer time for each tube diameter. The optimum is found for 1/16'' i.d. with a pump speed of 3400 rpm (≈ 650 mL.min^{-1}), which corresponds to a transfer time of 2.05 s for a 9.41 m distance.

Fig. 5 (b) shows the purity of the injected liquid in the NMR tube as a function of the speed of the pump. The purity is given by the volume fraction of H_2O. Here, we only show the results for the two bigger tube diameters. Indeed, no contamination could be detected for smaller i.d. This can be explained by two factors. First, smaller diameters limit the maximum speed of the pump due to higher pressure drops, thus decreasing the turbulences. Second, the length of the 3 mL plug of the loop pushed into the capillary is longer for smaller i.d. A longer plug length prevents the front of the plug from mixing with the driving liquid. However, for the two larger diameters, an unexpected behavior was observed. Indeed, for 1.4 mm i.d. the purity increases with the pump speed. For 1/16'' i.d., the purity starts by decreasing, then increases with the pump speed. In both cases, no contamination could be observed at their respective maximum speed. This phenomenon is explained in the literature [35,36] by the decreasing of the axial dispersion of the driving liquid in the driven liquid with high turbulence conditions. In return, it will decrease the mixing length. This turns out to be extraordinarily fortunate in our case, as choosing the faster transfer guarantees a maximal purity of the injected liquid in the NMR tube, despite the highly turbulent regime.

Performances of the system

The time taken by the whole process, from the start of the sequence to the NMR acquisition, can be split into four parts: (i) the time from the start of the sequence to the optical sensor detection, called t_{diss}, (ii) the time from the sensor detection to the start of the transfer that includes the response time of the system $t_{resp.}$ (8.4 ms) and the 10-way valve switching time t_{switch} (50 ms), (iii) the time from the start of the transfer to the end of injection, called $t_{transfer}$, and (iv) the time from the end of the injection to the triggering of the NMR acquisition that includes t_{switch} for the backpressure and t_{rest} for the liquid to stabilize. t_{diss} corresponds to the time taken by the gas-driven hot solvent to dissolve the sample and fill the loop. The total length of capillaries for this part is 6.68 m. It includes 2.79 m from the dissolution box to the sample cup, 1.98 m from the sample cup to the 10-way valve V1, 1.5 m for the loop and 41 cm from the end of the loop to the optical sensor. Six blank dissolutions were performed by freezing 100 μL of H_2O in liquid nitrogen, and using H_2O as the solvent (see the Methods section for details of the warm up parameters). t_{diss} was found to be 1351 ± 16 ms (risk = 5 %). This takes into account the first 2.79 m from the dissolution box to the sample cup, which does not contribute to the polarization losses due to liquid state

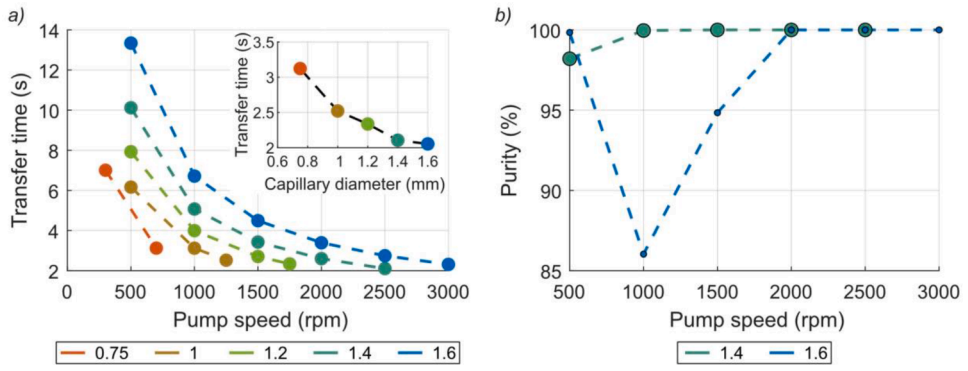

Fig. 5.. (a) transfer time of 3 mL of H_2O pushed by isopropanol through 9.41 m of capillary depending on the pump rotation speed, for the different capillary i.d. (from 0.75 mm to 1.6 mm). The upper right graph shows the shortest transfer time obtain for each capillary i.d. The different curves are just guides for the eye. – (b) Purity of the injected 540 µL sample (H_2O pushed by isopropanol) for 1/16'' (1.6 mm) and 1.4 mm i.d, depending on the pump speed. The purity is given by the volume fraction of H_2O in the injected liquid.

relaxation.

The transfer time $t_{transfer}$ corresponds to the liquid-driven transfer through the 9.44 m of capillary from the 10-way valve V1 to the NMR tube. Since the i.d. of the capillary and the driving liquid are fixed, $t_{transfer}$ depends only on the pump performances. For each turn of the pump gear, 192 µL of isopropanol is displaced. Here, the pump is set to turn 117 turns at a speed of 3750 rpm ($\approx$ 720 mL.min^{-1}), corresponding to a volume of 22.5 mL in a transfer time of 1.94 s. Note that the transfer time includes the acceleration and deceleration of the pump, set to be 1000 tr.s^{-2}. Also, we allow a slightly higher pressure for the pump here than for the results presented in Fig. 5, which allow us to increase the maximum speed of the pump. Finally, to account for the smaller inertia that can arise after switching off the pump, we chose $t_{transfer}$ to be 2.1 s in the automated sequence.

The time required for the injected sample to stabilize, t_{rest}, is also set in the automated sequence. Its value can be assessed by investigating the variation of the NMR spectral linewidths after the injection of a hyperpolarized sample. After polarizing the ^{13}C spins of 100 µL of the sample described in the Methods section, a dissolution was carried out, with the resting time t_{rest} set to be 0. A pseudo-2D acquisition was recorded with 5° flip-angle pulses every 5 s. Fig.6(a) shows the evolution of the linewidth of the ^{13}C-formate and 1-^{13}C-acetate peaks after injection. The first scan measured immediately after injection displays a line broadening larger than 8 Hz as shown in Fig. 6(b). However, starting from the second scan (5 s after the first scan), a stable linewidth smaller than 0.8 Hz is observed for both molecules. The other hyperpolarized solutes (1-^{13}C-alanine and ^{13}C-urea) have intrinsic broad NMR linewidth. Including the 50 ms necessary for 10-way valves to switch, the value for t_{rest} could safely be set to 5 s. Note that it would be of interest in the future to further optimize the resting time to be as short as possible without compromising the NMR resolution beyond what can be tolerated, depending on the application explored.

Finally, the hyperpolarized solution's temperature was not measured systematically but was estimated to be 29 °C by performing test experiments consisting in injecting the solution onto a Becker equipped with a temperature sensor.

DNP performances

The DNP parameters and sequences used here are described in Methods. Fig. 7(a) show the hyperpolarized ^{13}C decay over more than 6 min, for each ^{13}C-labeled compound of the sample. For each decay, a monoexponential fit is applied, as shown by the coloured lines. The first point was removed from the fit, since the first spectrum shows a rather poor linewidth as discussed in the previous section. This monoexponential fit was used to extract the ^{13}C longitudinal relaxation time constant T_1, as well as the ^{13}C polarization level P_0 at $t = 0$ s, ranging from 3.7 % to 4.3 %, presented in Fig. 7 (b). The measured concentration of each compound, using a ^{1}H thermal equilibrium and a reference spectrum acquired prior to the dissolution experiment, are also presented in Fig. 7 (b). A dilution factor of roughly 110 is observed. Note that the urea concentration could not be estimated by ^{1}H thermal equilibrium NMR, as the protons of urea rapidly exchange with the deuterium of the solvent.

Discussion

We presented here a dissolution and transfer system designed to push hyperpolarized samples in 2 s over 9.5 m of capillary. The system has demonstrated high robustness, with several hundreds of experiments performed without a single leakage or breakage ever observed during transfer and injection. Moreover, ^{13}C NMR linewidths below 0.8 Hz could be obtained within 5 s. The capillary i.d. and the pump parameters have been optimized to minimize the transfer time while ensuring no isopropanol contamination of the injected liquid. Optimizing transfer volume with a new capillary length typically takes one hour of work (five iterations) to reach the desired injected volume. Once this is done for one length, it is repeatable after switching back and forth to other

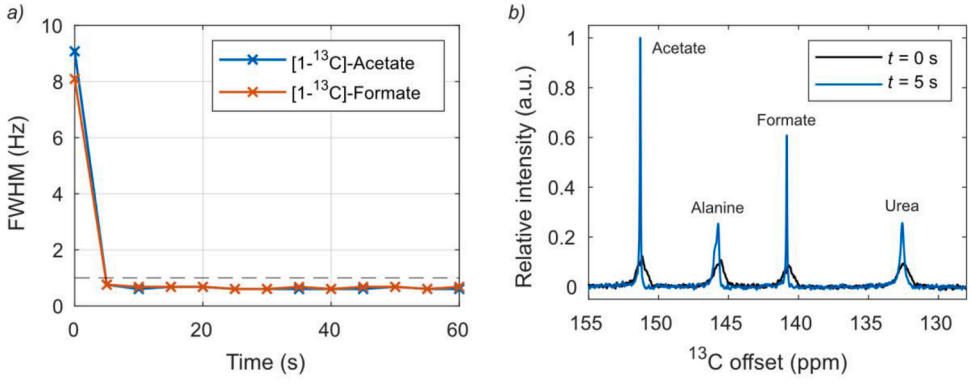

Fig. 6.. (a) Evolution of the full-width-at-half-maximum (FWHM) linewidth of the 1-^{13}C-acetate and ^{13}C-formate peaks after the injection of a hyperpolarized ^{13}C dissolved sample. One small flip-angle pulse and acquisition block was performed every 5 s. The dotted line indicates 1 Hz FWHM linewidth. Starting from the second point, the linewidth becomes stable at a value below 0.8 Hz. – (b) First and second spectra of the hyperpolarized injected sample, with peak assignment. The first spectrum shows a rather larger line broadening, assumed to be mainly due to fluid motion (note that the ppm scale is off by about -30 ppm as the lock was turned off prior to the injection of the hyperpolarized solution).

a)

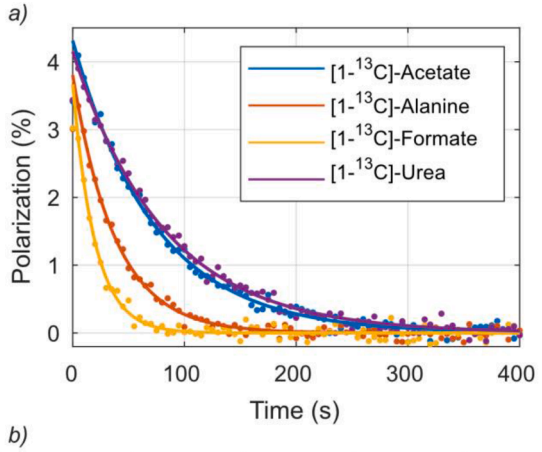

b)

Parameters	1-^{13}C-Acetate	^{13}C-Formate	1-^{13}C-Alanine	^{13}C-Urea
Polarization P_0 (%)	4.3 ± 0.1	3.7 ± 0.2	3.8 ± 0.1	4.2 ± 0.1
Relaxation time constant T_1 (s)	77.6 ± 2.3	20.2 ± 1.3	39.2 ± 1.6	87.2 ± 2.8
Concentration (mM)	0.94	0.82	1.02	/

Fig. 7.. (a) Hyperpolarized ^{13}C liquid-state relaxation of acetate, formate, alanine and urea following a dissolution experiment with the sample described in the Methods section to a Bruker Biospin Fourier 80 benchtop magnet. The coloured lines show the monoexponential fit. The fit was used to extract the ^{13}C longitudinal relaxation time constant T_1 and the polarization P_0 at $t = 0$ s. (b) P_0, T_1 and measured concentration of each compound. Due to proton/deuterium exchange, the urea concentration could not be measured.

lengths, and does not require further re-optimizations. This transfer system should in principle be compatible with *d*DNP experiments in any laboratory configuration, where the polarizer and NMR spectrometer can be several meters away from each other. This eases the coupling of one polarizer to several NMR spectrometers, which prevents dedicating a single magnet for the polarizer. However, such a transfer system is more complex than the classical gas-driven setup where the solution is simply pushed out of the sample cup directly to the NMR tube. In comparison, although our system should allow more precise injection volumes, it is still not fully automated as manual coupling of the dissolution stick is needed. Reaching improved repeatability can be essential for applications such as metabolomics [6]. Limiting human interventions during the dissolution steps is an important goal towards better repeatability as well as making *d*DNP more user friendly. Solutions exist, like the fluid path [37,38] designed for the SPINlab polarizer or the integrated sample cup and dissolution stick proposed by Capozzi et al., [39] and work in this direction is currently being conducted in our group. Another milestone is the concentration optimization of the injected liquid. Indeed, our average concentration of 0.93 mM in 540 μL of injected liquid indicates that only 5% of the 100 μL of sample arrived in the NMR tube. Although assessing repeatable concentrations is interesting for repeatability, decreasing the dilution factor will also ease the use of very lowly concentrated samples. Existing systems proposed to first gather the entire transferred plug in a reservoir above the NMR tube prior to the injection [9,34,40,41]. This ensures a homogeneous concentration of the sample in the whole solvent, and a better repeatability of the injected sample concentration. However, most of the sample stays in the solvent and is not injected with such a strategy. Another study showed that large samples could be dissolved in an efficient way if a nozzle was placed just at the end of the input capillary of the dissolution stick [42–44]. A fast and complete dissolution would induce a sharper concentration profile of the sample along the solvent plug length, leading to a higher injected sample quantity. Further optimizations of the dissolution efficiency and loop selection are under progress so as to maximize the amount of dissolved sample ultimately measured in the NMR spectrometer.

The obtained polarizations, ranging from 3.7% to 4.3% are lower than what can be found in the literature [9,45]. These polarization losses along the fluid path originate from passage through low magnetic field regions. Great care was taken regarding the magnetic field profile, with the addition of solenoids and a magnetic tunnel. Still, the solution passes through the 10-way valve, in which no solenoid can be placed. Stainless steel can sometimes be slightly magnetic and shield the surrounding magnetic field. By using a ceramic valve, we could tremendously improve the final polarization to $>$ 25%, at the cost of longer transfer time due to smaller acceptable pressure and longer switching time. In the future, we will implement a commercially available titanium variant of the fast-switching valve that will allow for high speed with identical transfer and injection performances, while preventing low field polarization losses.

We showed that, with fast transfers over long distances, fluidic dynamics cannot be neglected. Such dynamics, rarely described in the NMR and DNP literature, make gas-driven transfer and injection hardly precise and repeatable. Liquid-driven transfer induces mixing between liquids that can contaminate the injected volume. However, as shown in this experimental study, higher transfer speed, and thus higher turbulences, can limit the axial dispersion and ultimately the contamination. Simulations based on theoretical or empirical models could further help decreasing transfer times by optimizing parameters *in silico*, such as the length and i.d. of the loop capillary, the inner diameter of the 10-way valve, and more importantly the physical properties of the driving liquid. Indeed, a non-miscible liquid could additionally help preventing mixing. Viscosity and density also play an important role. Optimizing all such parameters experimentally would be excessively long, and preliminary simulations are currently in progress.

Conclusion

We have presented a liquid-driven transfer and injection system that enables contamination free hyperpolarized sample transfers at high speed (5 m.s^{-1}) and without contamination (nor driving liquid, nor bubbles). NMR linewidths less than 0.8 Hz are measured after injection and stabilization of the sample. Further improvements are foreseen to improve the overall performance, in particular lower polarization losses by using titanium rather than stainless-steel as the valve material. We believe this system will be suitable for a range of applications, such as metabolomics or drug screening, that typically require such speed to prevent polarization losses of fast relaxing nuclear spins. Further studies of the repeatability (volume, concentration, polarization) and stability (at short times t_{rest} below 5 s) with this high-speed and contamination free transfer system will be carried on in the future.

Declaration of Competing Interest

The authors declare that they have no known competing financial interests or personal relationships that could have appeared to influence the work reported in this paper.

Acknowledgments

This research was supported by ENS-Lyon, the French CNRS, Lyon 1 University, the European Research Council under the European Union's Horizon 2020 research and innovation program (ERC Grant Agreements No. 714519 / HP4all and Marie Skłodowska-Curie Grant Agreement No. 766402 / ZULF). The authors gratefully acknowledge Bruker Biospin for providing the prototype *d*DNP polarizer, and particularly Roberto Melzi, Marc Rossire, Marco Sacher and Marc Schnell for scientific and technical support. The authors graciously acknowledge Frank Decker, Bruno Knittel and Venita Decker for lending assistance with the operation of

the permanent magnet Bruker Biospin Fourier 80 benchtop NMR system. The authors additionally acknowledge Stéphane Martinez of the UCBL mechanical workshop for machining parts of the experimental apparatus; and Paul-Emmanuel Edeline for assisting with dissolution experiments.

References

[1] R.A.K. Nadkarni, J.C. Edwards, A review of applications of NMR spectroscopy in the petroleum industry. Spectroscopic Analysis of Petroleum Products and Lubricants, ASTM International, 2011, https://doi.org/10.1520/MONO10117M, 423-423–50 100 Barr Harbor Drive, PO Box C700, West Conshohocken, PA 19428-2959.

[2] U. Bussy, M. Boujtita, Review of advances in coupling electrochemistry and liquid state NMR, Talanta 136 (2015) 155–160, https://doi.org/10.1016/j.talanta.2014.08.033.

[3] H. Hiroaki, Application of NMR in drug discovery, Nucl. Magn. Reson. 45 (2016) 217–239, https://doi.org/10.1039/9781782624103-00217.

[4] E. Hatzakis, Nuclear magnetic resonance (NMR) Spectroscopy in food science: a comprehensive review, Compr. Rev. Food Sci. Food Saf. 18 (2019) 189–220, https://doi.org/10.1111/1541-4337.12408.

[5] J. Kruk, M. Doskocz, E. Jodłowska, A. Zacharzewska, J. Łakomiec, K. Czaja, J. Kujawski, NMR techniques in metabolomic studies: a quick overview on examples of utilization, Appl. Magn. Reson. 48 (2017) 1–21, https://doi.org/10.1007/s00723-016-0846-9.

[6] A. Dey, B. Charrier, E. Martineau, C. Deborde, E. Gandriau, A. Moing, D. Jacob, D. Eshchenko, M. Schnell, R. Melzi, D. Kurzbach, M. Ceillier, Q. Chappuis, S. F. Cousin, J.G. Kempf, S. Jannin, J.-N. Dumez, P. Giraudeau, Hyperpolarized NMR metabolomics at natural ^{13}C abundance, Anal. Chem. 92 (2020) 14867–14871, https://doi.org/10.1021/acs.analchem.0c03510.

[7] K.V. Kovtunov, E.V. Pokochueva, O.G. Salnikov, S.F. Cousin, D. Kurzbach, B. Vuichoud, S. Jannin, E.Y. Chekmenev, B.M. Goodson, D.A. Barskiy, I.V. Koptyug, Hyperpolarized NMR Spectroscopy: d-DNP, PHIP, and SABRE techniques, Chem. Asian J. 13 (2018) 1857–1871, https://doi.org/10.1002/asia.201800551.

[8] J.H. Ardenkjaer-Larsen, B. Fridlund, A. Gram, G. Hansson, L. Hansson, M. H. Lerche, R. Servin, M. Thaning, K. Golman, Increase in signal-to-noise ratio of > 10,000 times in liquid-state NMR, Proc. Natl. Acad. Sci. U. S. A. 100 (2003) 10158–10163, https://doi.org/10.1073/pnas.1733835100.

[9] S. Jannin, A. Bornet, R. Melzi, G. Bodenhausen, High field dynamic nuclear polarization at 6.7 T: carbon-13 polarization above 70% within 20 min, Chem. Phys. Lett. 549 (2012) 99–102, https://doi.org/10.1016/j.cplett.2012.08.017.

[10] M. Cavaillès, A. Bornet, X. Jaurand, B. Vuichoud, D. Baudouin, M. Baudin, L. Veyre, G. Bodenhausen, J.-N. Dumez, S. Jannin, C. Copéret, C. Thieuleux, Tailored microstructured hyperpolarizing matrices for optimal magnetic resonance imaging, Angew. Chem. Int. Ed. 57 (2018) 7453–7457, https://doi.org/10.1002/anie.201801009.

[11] A.C. Pinon, A. Capozzi, J.H. Ardenkjær-Larsen, Hyperpolarized water through dissolution dynamic nuclear polarization with UV-generated radicals, Commun. Chem. 3 (2020) 1–9, https://doi.org/10.1038/s42004-020-0301-6, 2020 31.

[12] H. Jóhannesson, S. Macholl, J.H. Ardenkjaer-Larsen, Dynamic Nuclear Polarization of [1-^{13}C]pyruvic acid at 4.6 tesla, J. Magn. Reson. 197 (2009) 167–175, https://doi.org/10.1016/j.jmr.2008.12.016.

[13] A. Capozzi, S. Patel, W.T. Wenckebach, M. Karlsson, M.H. Lerche, J.H. Ardenkjær-Larsen, Gadolinium effect at high-magnetic-field DNP: 70% ^{13}C polarization of [U-^{13}C] glucose using trityl, J. Phys. Chem. Lett. 10 (2019) 3420–3425, https://doi.org/10.1021/acs.jpclett.9b01306.

[14] A. Bornet, A. Pinon, A. Jhajharia, M. Baudin, X. Ji, L. Emsley, G. Bodenhausen, J. H. Ardenkjaer-Larsen, S. Jannin, Microwave-gated dynamic nuclear polarization, Phys. Chem. Chem. Phys. 18 (2016) 30530–30535, https://doi.org/10.1039/c6cp05587g.

[15] A.S. Kiryutin, B.A. Rodin, A.V. Yurkovskaya, K.L. Ivanov, D. Kurzbach, S. Jannin, D. Guarin, D. Abergel, G. Bodenhausen, Transport of hyperpolarized samples in dissolution-DNP experiments, Phys. Chem. Chem. Phys. 21 (2019) 13696–13705, https://doi.org/10.1039/C9CP02600B.

[16] K. Miesel, K.L. Ivanov, A.V. Yurkovskaya, H.M. Vieth, Coherence transfer during field-cycling NMR experiments, Chem. Phys. Lett. 425 (2006) 71–76, https://doi.org/10.1016/j.cplett.2006.05.025.

[17] J. Eills, J.W. Blanchard, T. Wu, C. Bengs, J. Hollenbach, D. Budker, M.H. Levitt, Polarization transfer via field sweeping in parahydrogen-enhanced nuclear magnetic resonance, J. Chem. Phys. 150 (2019), 174202, https://doi.org/10.1063/1.5089486.

[18] P. Berthault, C. Boutin, C. Martineau-Corcos, G. Carret, Use of dissolved hyperpolarized species in NMR: practical considerations, Prog. Nucl. Magn. Reson. Spectrosc. 118–119 (2020) 74–90, https://doi.org/10.1016/j.pnmrs.2020.03.002.

[19] J. Granwehr, R. Panek, J. Leggett, W. Köckenberger, Quantifying the transfer and settling in NMR experiments with sample shuttling, J. Chem. Phys. 132 (2010), 244507, https://doi.org/10.1063/1.3446804.

[20] T. Harris, C. Bretschneider, L. Frydman, Dissolution DNP NMR with solvent mixtures: substrate concentration and radical extraction, J. Magn. Reson. 211 (2011) 96–100, https://doi.org/10.1016/j.jmr.2011.04.001.

[21] S. Bowen, C. Hilty, Rapid sample injection for hyperpolarized NMR spectroscopy, Phys. Chem. Chem. Phys. 12 (2010) 5766–5770, https://doi.org/10.1039/c002316g.

[22] S. Katsikis, I. Marin-Montesinos, M. Pons, C. Ludwig, U.L. Günther, Improved stability and spectral quality in *ex situ* dissolution DNP using an improved transfer device, Appl. Magn. Reson. 46 (2015) 723–729, https://doi.org/10.1007/s00723-015-0680-5.

[23] G. Olsen, E. Markhasin, O. Szekely, C. Bretschneider, L. Frydman, Optimizing water hyperpolarization and dissolution for sensitivity-enhanced 2D biomolecular NMR, J. Magn. Reson. 264 (2016) 49–58, https://doi.org/10.1016/j.jmr.2016.01.005.

[24] H.Y. Chen, C. Hilty, Implementation and characterization of flow injection in dissolution dynamic nuclear polarization NMR spectroscopy, ChemPhysChem 16 (2015) 2646–2652, https://doi.org/10.1002/cphc.201500292.

[25] H.Y. Chen, C. Hilty, Hyperpolarized Hadamard spectroscopy using flow NMR, Anal. Chem. 85 (2013) 7385–7390, https://doi.org/10.1021/ac401293n.

[26] Y. Lee, H. Zeng, A. Mazur, M. Wegstroth, T. Carlomagno, M. Reese, D. Lee, S. Becker, C. Griesinger, C. Hilty, Hyperpolarized binding pocket nuclear overhauser effect for determination of competitive ligand binding, Angew. Chem. Int. Ed. 51 (2012) 5179–5182, https://doi.org/10.1002/anie.201201003.

[27] H.Y. Chen, Y. Lee, S. Bowen, C. Hilty, Spontaneous emission of NMR signals in hyperpolarized proton spin systems, J. Magn. Reson. 208 (2011) 204–209, https://doi.org/10.1016/j.jmr.2010.11.002.

[28] H. Fujioka, J.B. Grotberg, The steady propagation of a surfactant-laden liquid plug in a two-dimensional channel, Phys. Fluids. 17 (2005) 1–17, https://doi.org/10.1063/1.1948907.

[29] J. Kim, J.D. O'Neill, N.V. Dorrello, M. Bacchetta, G. Vunjak-Novakovic, Targeted delivery of liquid microvolumes into the lung, Proc. Natl. Acad. Sci. 112 (2015) 11530–11535, https://doi.org/10.1073/pnas.1512613112.

[30] K.J. Cassidy, N. Gavriely, J.B. Grotberg, Liquid Plug flow in straight and bifurcating tubes, J. Biomech. Eng. 123 (2002) 580, https://doi.org/10.1115/1.1406949.

[31] J.C. Magniez, M. Baudoin, C. Liu, F. Zoueshtiagh, Dynamics of liquid plugs in prewetted capillary tubes: from acceleration and rupture to deceleration and airway obstruction, Soft Matter 12 (2016) 8710–8717, https://doi.org/10.1039/c6sm01463a.

[32] L. Zhao, J. Derksen, R. Gupta, Simulations of axial mixing of liquids in a long horizontal pipe for industrial applications, Energy and Fuels 24 (2010) 5844–5850, https://doi.org/10.1021/ef100846r.

[33] J. Milani, B. Vuichoud, A. Bornet, P. Miéville, R. Mottier, S. Jannin, G. Bodenhausen, A magnetic tunnel to shelter hyperpolarized fluids, Rev. Sci. Instrum. (2015) 86, https://doi.org/10.1063/1.4908196.

[34] A. Bornet, R. Melzi, A.J. Perez Linde, P. Hautle, B. Van Den Brandt, S. Jannin, G. Bodenhausen, Boosting dissolution dynamic nuclear polarization by cross polarization, J. Phys. Chem. Lett. 4 (2013) 111–114, https://doi.org/10.1021/jz301781t.

[35] A.R. Patrachari, A.H. Johannes, A conceptual framework to model interfacial contamination in multiproduct petroleum pipelines, Int. J. Heat Mass Transf. 55 (2012) 4613–4620, https://doi.org/10.1016/j.ijheatmasstransfer.2012.04.017.

[36] G. He, M. Lin, B. Wang, Y. Liang, Q. Huang, Experimental and numerical research on the axial and radial concentration distribution feature of miscible fluid interfacial mixing process in products pipeline for industrial applications, Int. J. Heat Mass Transf. 127 (2018) 728–745, https://doi.org/10.1016/j.ijheatmasstransfer.2018.08.080.

[37] J.H. Ardenkjaer-Larsen, A.M. Leach, N. Clarke, J. Urbahn, D. Anderson, T. W. Skloss, Dynamic nuclear polarization polarizer for sterile use intent, NMR Biomed. 24 (2011) 927–932, https://doi.org/10.1002/nbm.1682.

[38] R.M. Malinowski, K.W. Lipsø, M.H. Lerche, J.H. Ardenkjær-Larsen, Dissolution dynamic nuclear polarization capability study with fluid path, J. Magn. Reson. 272 (2016) 141–146, https://doi.org/10.1016/j.jmr.2016.09.015.

[39] A. Capozzi, M. Karlsson, J.R. Petersen, M.H. Lerche, J.H. Ardenkjaer-Larsen, Liquid-state ^{13}C Polarization of 30% through photoinduced nonpersistent radicals, J. Phys. Chem. C. 122 (2018) 7432–7443, https://doi.org/10.1021/acs.jpcc.8b01482.

[40] A. Bornet, M. Maucourt, C. Deborde, D. Jacob, J. Milani, B. Vuichoud, X. Ji, J. N. Dumez, A. Moing, G. Bodenhausen, S. Jannin, P. Giraudeau, Highly repeatable dissolution dynamic nuclear polarization for heteronuclear NMR metabolomics, Anal. Chem. 88 (2016) 6179–6183, https://doi.org/10.1021/acs.analchem.6b01094.

[41] X. Ji, A Bornet, B. Vuichoud, J. Milani, D. Gajan, A.J. Rossini, L. Emsley, G. Bodenhausen, S. Jannin, Transportable hyperpolarized metabolites, Nat. Commun. 8 (2017) 13975, https://doi.org/10.1038/ncomms13975.

[42] J. Jain, S. Dey, L. Muralidharan, A.M. Leach, J.H. Ardenkjaer-Larsen, Jet impingement melting with vaporization: a numerical study, in: Proceedings of the ASME 2008 Heat Transfer Summer Conference collocated with the Fluids Engineering, Energy Sustainability, and 3rd Energy Nanotechnology Conferences 2, ASMEDC, 2008, pp. 559–567, https://doi.org/10.1115/HT2008-56148.

[43] N. (US) Jan Henrik Ardenkjaer-larsen, Amersham (GB); David Dietrich, Niskayuna, NY (US); Karl Andreas Gram, Oslo (NO); Andrew M. Leach, Clifton Park, NY (US); Peter Miller, New London, CT (US); Eric J. Telfeyan, Guilderland, NY (US); Mikkel Thaning, Oslo (NO); Da, Patent - NOZZLE FOR DNP POLARIZER, 1 (2011) 739–740.

[44] S. Bowen, J.H. Ardenkjaer-Larsen, Enhanced performance large volume dissolution-DNP, J. Magn. Reson. 240 (2014) 90–94, https://doi.org/10.1016/j.jmr.2014.01.009.

[45] J.H. Ardenkjær-Larsen, S. Bowen, J.R. Petersen, O. Rybalko, M.S. Vinding, M. Ullisch, N.C. Nielsen, Cryogen-free dissolution dynamic nuclear polarization polarizer operating at 3.35 T, 6.70 T, and 10.1 T, Magn. Reson. Med. 81 (2019) 2184–2194, https://doi.org/10.1002/mrm.27537.

[46] Elliott S. J., Stern Q., Ceillier M., El Daraï T., Cousin S. F., Cala O., Jannin S., Practical dissolution dynamic nuclear polarization, Progress in Nuclear Magnetic Resonance Spectroscopy ISSN 0079-6565 Volumes2021 (126–127) 59–https://doi.org/10.1016/j.pnmrs.2021.04.002.